BMAA and MCLR Interact to Modulate Behavior and Exacerbate Molecular Changes Related to Neurodegeneration in Larval Zebrafish

Rubia M. Martin, Michael S. Bereman, and Kurt C. Marsden [1]

Department of Biological Sciences, North Carolina State University, Raleigh, North Carolina 27695, USA

[1]To whom correspondence should be addressed. E-mail: kcmarsde@ncsu.edu.

ABSTRACT

Exposure to toxins produced by cyanobacteria (ie, cyanotoxins) is an emerging health concern due to their increasing prevalence and previous associations with neurodegenerative diseases including amyotrophic lateral sclerosis. The objective of this study was to evaluate the neurotoxic effects of a mixture of two co-occurring cyanotoxins, β-methylamino-L-alanine (BMAA) and microcystin leucine and arginine (MCLR), using the larval zebrafish model. We combined high-throughput behavior-based toxicity assays with discovery proteomic techniques to identify behavioral and molecular changes following 6 days of exposure. Although neither toxin caused mortality, morphological defects, nor altered general locomotor behavior in zebrafish larvae, both toxins increased acoustic startle sensitivity in a dose-dependent manner by at least 40% ($p < .0001$). Furthermore, startle sensitivity was enhanced by an additional 40% in larvae exposed to the BMAA/MCLR mixture relative to those exposed to the individual toxins. Supporting these behavioral results, our proteomic analysis revealed a 4-fold increase in the number of differentially expressed proteins in the mixture-exposed group. Additionally, prediction analysis reveals activation and/or inhibition of 8 enriched canonical pathways (enrichment p-value $< .01$; z-score $\geq |2|$), including ILK, Rho Family GTPase, RhoGDI, and calcium signaling pathways, which have been implicated in neurodegeneration. We also found that expression of TDP-43, of which cytoplasmic aggregates are a hallmark of amyotrophic lateral sclerosis pathology, was significantly upregulated by 5.7-fold following BMAA/MCLR mixture exposure. Together, our results emphasize the importance of including mixtures of cyanotoxins when investigating the link between environmental cyanotoxins and neurodegeneration as we reveal that BMAA and MCLR interact *in vivo* to enhance neurotoxicity.

Key words: cyanotoxins; mixtures; zebrafish; behavior; proteomics.

Amyotrophic lateral sclerosis (ALS) is the most common neurodegenerative disease of midlife and is rapidly fatal with a median survival period of 3 years from symptom onset (Brown and Al-Chalabi, 2017). It is defined by a progressive loss of both upper and lower motor neurons, resulting in muscle spasticity, weakness, and atrophy (Swinnen and Robberecht, 2014). Approximately 10% of ALS cases are classified as familial due to the inheritance of single gene mutations (Renton et al., 2014). For the remaining 90% of cases, the disease etiology is unknown and likely stems from a complex interplay between genetic and environmental factors (Ingre et al., 2015; Jones, 2009). Although

the contribution of environmental factors to sporadic ALS (sALS) is difficult to assess as the search space is infinite, several studies have associated ALS incidence with exposure to heavy metals, pesticides, and electromagnetic fields (reviewed in Bozzoni, 2016). In addition, there is strong evidence that exposure to cyanotoxins is a major risk factor for sALS (Bradley and Mash, 2009).

The link between beta-methylamino-L-alanine (BMAA), a toxin produced by a diverse taxa of cyanobacteria (Cox et al., 2005), and sALS was first observed on the island of Guam in the 1950s (Kurland and Mulder, 1955). The indigenous population of

Guam succumbed to an ALS/parkinsonism-dementia (PD) neurodegenerative complex with a 100-fold greater incidence than the rest of the world (Bradley and Mash, 2009). The elevated rates of ALS/PD in Guam were attributed to BMAA exposure as the indigenous population consumed flour made from BMAA-containing cycad seeds as well as flying foxes in which BMAA was biomagnified up to 10,000-fold greater than in free living bacteria (3556 μg/g BMAA) (Banack and Cox, 2003). Several studies have since implicated BMAA in sALS cases outside of Guam, including clusters of ALS along the French Mediterranean coast, New Hampshire, and Maryland (Caller *et al.*, 2009; Field *et al.*, 2013; Masseret *et al.*, 2013). These epidemiological studies provide evidence that exposure to BMAA is associated with neurodegeneration. Epidemiological findings are further supported by laboratory studies in which BMAA was found to cause neurotoxic effects consistent with neurodegenerative disease (Beri *et al.*, 2017; Karlsson *et al.*, 2017). Furthermore, neonatal BMAA exposure in rats has been shown to produce motor defects (Scott *et al.*, 2017), indicating that exposure during neural development may enhance sALS risk. However, a major limitation for these and many other BMAA studies is that BMAA is just one of many toxic metabolites produced by cyanobacteria, some of which have been reported to co-occur with BMAA around the world (Banack *et al.*, 2015; Sabart *et al.*, 2015). Thus, to obtain a more thorough understanding of the risk posed by exposure to cyanotoxic blooms, it is essential to investigate the toxicity of other cyanotoxins with BMAA.

BMAA at low concentrations (∼10 μM) in combination with other non-cyanotoxic neurotoxins has been found to potentiate neuronal damage *in vitro* (Lobner *et al.*, 2007). More recently, our laboratory demonstrated that co-exposure to BMAA and its isomers AEG and 2,4DAB at 166 μM (total concentration 500 μM) produces a synergistic interaction *in vitro*, reducing viability of motor neuron-like NSC-34 cells and perturbing regulation of various canonical pathways, bioprocesses, and upstream regulators involved in neurodegeneration (Martin *et al.*, 2019). Although widely known as a hepatotoxin, microcystin leucine-arginine (MCLR) is also a potent neurotoxin, as demonstrated in multiple species including nematodes, zebrafish, birds, and mammals (Li *et al.*, 2009; Pašková *et al.*, 2008; Tzima, 2017; Zhao *et al.*, 2015). Microcystins are the most abundant cyanotoxins in the environment and have been shown to co-occur with BMAA at levels ranging from ng·l^{-1} to μg·l^{-1} concentrations (Banack *et al.*, 2015; Jungblut *et al.*, 2018; Metcalf *et al.*, 2012), and like BMAA, MCLR can bioaccumulate in tissues (Wang *et al.*, 2008; Zhao *et al.*, 2015). Previously, BMAA and MCLR have been detected together in 7 of 12 waterbodies analyzed in the United Kingdom (Metcalf *et al.*, 2008). Therefore, co-exposure to BMAA and MCLR is of increasing toxicological significance.

To identify potential neurotoxic effects *in vivo*, we exposed larval zebrafish to BMAA and/or MCLR and assessed neural function by analyzing changes in behavior using a high-throughput testing platform. We tested both spontaneous locomotion and acoustic startle responses as both behaviors require proper motor function, and defects in these assays would indicate dysfunction within the underlying motor circuits, thus giving them direct relevance to motor neuron diseases such as ALS. Indeed, spontaneous locomotion has been used to validate several zebrafish motor neuron disease models including for ALS and spinal muscular atrophy (SMA) (Ciura *et al.*, 2013; Hao *et al.*, 2012; McGown *et al.*, 2013; Ramesh *et al.*, 2010). The startle response is a rapid, high-velocity movement that requires coordinated activation of motor neurons in every segment of the fish's body. Furthermore, sensory defects are also found in ALS

cases (Tao *et al.*, 2018), so the startle assay provides an opportunity to probe both sensory and motor dysfunction in cyanotoxin-exposed larvae. Although neither BMAA nor MCLR caused changes in locomotion, both toxins increased acoustic startle sensitivity in a dose-dependent manner. Furthermore, a mixture of BMAA and MCLR enhanced toxicity in the startle assay. Finally, we examined the protein profile of larval zebrafish exposed to the BMAA/MCLR mixture and identified molecular signatures consistent with neurodegeneration, including upregulation of the ALS-associated protein TDP-43 (Mackenzie *et al.*, 2010). Together, our data highlight the importance of studying toxic mixtures and reveal novel mechanisms that may link cyanotoxin exposure to motor diseases such as sALS.

MATERIALS AND METHODS

Chemicals
Synthetic BMAA standards were obtained from Sigma Aldrich (St Louis, Missouri), and purified MCLR (purity >95%) was obtained from Enzo Life Sciences, Inc. (Farmingdale, New York). Water, acetonitrile, methanol, acetic acid, and formic acid were all Optima LC–MS-grade solvents purchased from Fisher Scientific (Tewksbury, Massachusetts). A stock solution of BMAA at 10 mg·ml^{-1} and MCLR at 1 mg·ml^{-1} was used for all dilutions. All BMAA dilutions were prepared in high-performance liquid chromatography (HPLC)-grade water while MCLR dilutions were prepared in DMSO (Fisher Scientific).

Zebrafish Husbandry and Exposures
All animal use and procedures were approved by the North Carolina State University IACUC. Zebrafish (*Danio rerio*) embryos from multiple crosses of wild-type tupfel longfin (TLF) strain adults were collected and placed into Petri dishes containing E3 medium, and unfertilized eggs were removed as described previously (Burgess and Granato, 2007). Embryos from all clutches were mixed and randomly sorted into 24 well plates (8–10 animals per well) containing 1 ml of E3 per well.

At 6 hpf, all E3 was removed and replaced with vehicle (HPLC-grade water), 100, 500, or 1000 μM BMAA in E3, vehicle (DMSO), 1, 2.5, 5, or 10 μM MCLR in E3, or 100 μM BMAA plus 1 μM MCLR in E3. All treatments were performed in triplicate and were repeated in each of 3 separate experiments. Embryos were incubated at 29°C on a 14 h:10 h light-dark cycle, and 100% of the media was exchanged for fresh solutions daily. During media changes, each fish was assessed for a set of developmental phenotypes (pericardial edema, otolith malformations, pigmentation defects, small eyes, small heads, body axis defects such as curved or bent tails, and uninflated swim bladders), and any fish exhibiting these phenotypes was removed. Embryos/larvae were exposed to treatments until 6 days post fertilization (6 dpf).

Behavior Assays and Analysis
Screened larvae were adapted to the testing lighting and temperature conditions for 30 min prior to testing. Behavior testing was done as described previously (Burgess and Granato, 2007; Marsden *et al.*, 2018). Briefly, 6 dpf larvae were transferred to individual 9 mm round wells on a 36-well laser-cut acrylic testing grid. Larvae acclimated for 5 min and then spontaneous locomotor activity was recorded for 18.5 min at 640 × 640 px resolution at 50 frames per sec (fps) using a Photron mini UX-50 high-speed camera. The same set of larvae were then presented with a total of 60 acoustic stimuli, 10 at each of 6 intensities (13.6,

25.7, 29.2, 35.5, 39.6, and 53.6 dB), with a 20-s interstimulus interval (ISI). Startle responses were recorded at 1000 fps. Stimuli were delivered by an acoustic-vibrational shaker (Bruel and Kjaer) to which the testing grid was directly mounted. All stimuli were calibrated with a PCB Piezotronics accelerometer (no. 355B04) and signal conditioner (no. 482A21), and voltage outputs were converted to dB using the formula $dB = 20 \log V$. Analysis of recorded behaviors was done using FLOTE software as described previously (Burgess and Granato, 2007; Marsden et al., 2018). Short-latency C-bends (SLCs) and long-latency C-bends (LLCs) were determined by defined kinematic parameters. A startle sensitivity index was calculated for individual larvae by calculating the area under the curve of startle frequency versus stimulus intensity using Prism 8 software (GraphPad). Statistical analyses were performed using JMP pro 14 from SAS Institute, Cary, North Carolina. Data were analyzed for effects between the groups (comparison of means), using Tukey-Kramer HSD, Alpha 0.05. Violin plots were generated using Prism 8. All testing and analysis was performed blind to the treatment condition, with the data decoded only at the completion of the experiment. All behavioral data are available upon request to the corresponding author.

Proteomics Analysis

Sample preparation and LC MS/MS. Details of sample preparation, protein extraction, and digestion via filter-aided sample preparation (FASP) can be found in Supplemental Methods. Details regarding the high-pressure liquid chromatography combined mass spectrometry (LC-MS)/MS data collection are also provided in the Supplemental Methods. Raw data files obtained in this experiment have been made available on the Chorus LC-MS data repository and can be assessed under the project ID1679.

Proteomics data analysis. Details for the label-free quantitation (LFQ) have been previously described here (Martin et al., 2019). In brief, LFQ was performed in MaxQuant (version.1.5.60), and data were searched against the *Danio rerio* Swiss Prot protein database (no. of protein sequences = 56 281, accessed March 22, 2019). Comparison of LFQ intensities across the whole set of measurements was investigated using Perseus software (version 1.5.1.6), where calculation of statistical significance was determined using two-way Student t test and FPR ($p \leq .05$).

Pathway analysis. Ingenuity pathway analysis (IPA) software was used to identify the function, specific processes, and enriched pathways of the differentially expressed proteins (DEPs) using the "Core Analysis" function. Only significantly DEPs ($p \leq .05$) were submitted to IPA. We used an empirical background protein database to evaluate the significance of pathway enrichment. The database was created by using all of the proteins that were detected in our samples (Bereman et al., 2018; Khatri and Drăghici, 2005).

RESULTS

An overview of the experimental design is illustrated in Figure 1. In brief, we first conducted a dose-response study to determine the no observed adverse effect levels (NOAELs) to be implemented in subsequent mixture analyses. Zebrafish larvae were exposed to increasing concentrations of BMAA or MCLR from 6 hours post-fertilization (hpf) to 6 days post-fertilization (dpf). At 6 dpf, neurotoxicity was evaluated via two behavioral assays: spontaneous locomotion and acoustic startle response

analysis. Based on these data, a mixture was created using BMAA and MCLR at their respective NOAELs in which zebrafish larvae were exposed as before, followed by behavior analysis to identify potential interactions between BMAA and MCLR. Finally, to investigate perturbed molecular pathways associated with cyanotoxic mixture exposure, the mixture-exposed group and their respective controls were subjected to shotgun proteomics.

BMAA and MCLR Dose-Response Study: Identification of NOAELs

To determine if exposure to environmentally relevant concentrations of BMAA or MCLR cause neurotoxicity in wild-type zebrafish, we treated TLF strain embryos from 6 hpf to 6 dpf with increasing concentrations of BMAA (100, 500, and 1000 μM) and MCLR (1, 2.5, 5, and 10 μM). As the mass of each group of approximately nine zebrafish larvae is 0.5 mg, these concentrations are equivalent to 2.36–23.6 mg.g^{-1} BMAA and 0.2–2 mg.g^{-1} MCLR of dry weight, comparable to levels found in environmental samples (Lance et al., 2018; Sahin et al., 1996). We did not observe increased mortality or any overt developmental phenotypes including uninflated swim bladder, pericardial edema, otolith defects, pigmentation changes, small eyes, or body axis defects such as bent tails in any of the exposed groups of larvae. First, we examined the effect of BMAA and MCLR on general locomotion (Figure 2) using a custom built, high-throughput behavior platform and unbiased, automated FLOTE tracking and analysis software (Burgess and Granato, 2007). In order to investigate if various concentrations of BMAA and/or MCLR could alter spontaneous movement, 6 dpf larvae were adapted to the testing conditions for 30 min, transferred to a multi-well grid mounted below a high-speed camera, habituated for 5 additional minutes, and then their spontaneous movements were recorded for 18.5 min. We detected no significant differences in total distance travelled for zebrafish larvae treated with either BMAA or MCLR compared with their respective vehicle controls (Figure 2A). Average speed was also unchanged in all groups, except for larvae treated with 1000 μM BMAA, whose speed was significantly reduced (Figure 2B). We also examined the frequency of turning and swimming behaviors, as defined by specific kinematic parameters (Hao et al., 2012). There were no significant differences in the ratio of turns to swims in BMAA or MCLR treated larvae (Figure 2C). The overall frequency of these movements was also unchanged, except for a slight increase in turn frequency in 10 μM MCLR-treated larvae (Supplementary Figure 1). These data indicate that developmental exposure to BMAA or MCLR does not substantially affect general locomotor activity in larval zebrafish.

We then we examined sensorimotor function using an acoustic startle assay consisting of 60 total stimuli, 10 at each of 6 intensities with a 20-s inter-stimulus interval (Figure 3). In response to an acoustic stimulus, zebrafish larvae perform one of two types of high-velocity startle behaviors: SLCs, which rely on the Mauthner neurons (Burgess and Granato, 2007), or LLCs, which are independent of the Mauthner cells but require a set of prepontine neurons (Marquart et al., 2019). To investigate if BMAA or MCLR alters startle performance, we measured SLC and LLC frequency across the 60-stimulus assay (Figure 3). Figure 3A highlights both the SLC and LLC response frequency disparities between zebrafish larvae exposed to 1000 μM BMAA and vehicle control. 1000 μM BMAA increases SLC responses while decreasing LLC responses, indicating that BMAA shifts the behavioral response bias toward SLCs.
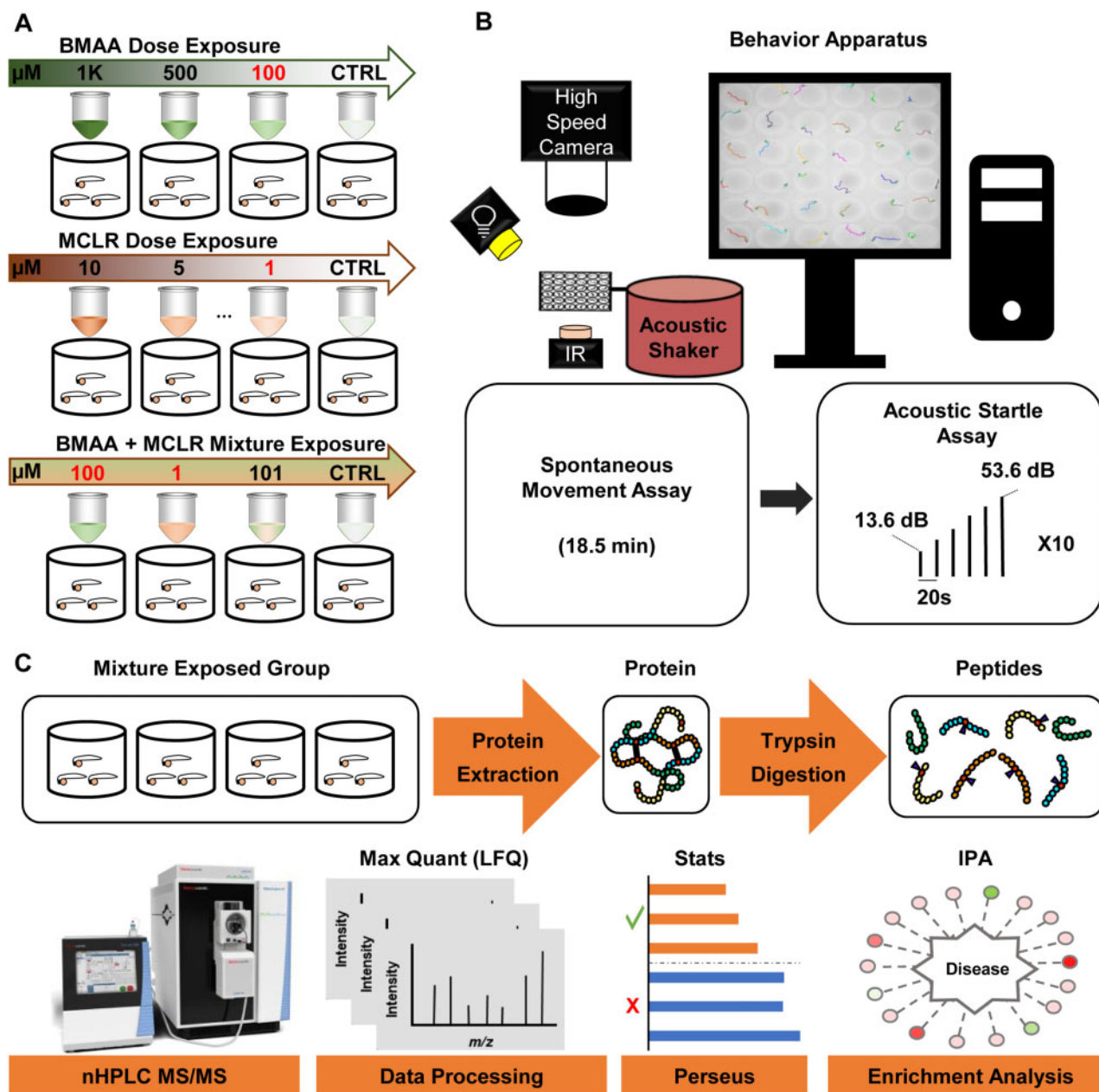
Figure 1. Experimental design. A, Cyanotoxin exposure plan for zebrafish from 6 hpf to 6 dpf. B, High-throughput behavior testing apparatus: multi-well testing grid is mounted on an acoustic shaker above an infrared (IR) LED array and below an IR-sensitive high-speed camera. A white LED is mounted above the grid to simulate daylight conditions. Videos are analyzed with automated tracking software (FLOTE). C, Proteomics workflow: zebrafish larvae from the mixture exposed groups were pooled for protein extraction and tryptic digestion of extracted proteins into peptides. nLC-MS/MS label-free protein quantitation via MaxQuant statistical analysis via Perseus software and enrichment analysis via ingenuity pathway analysis (IPA).

To quantify SLC and LLC sensitivity, we calculated the area under the startle frequency curves in Figure 3A for each individual larva to create a startle sensitivity index (Marsden *et al.*, 2018). Both BMAA and MCLR increased SLC sensitivity in a dose-dependent manner (Figure 3B). LLC responses decreased in a dose-dependent manner in both BMAA and MCLR-treated larvae, supporting an overall shift in response bias (Figure 3C). These data indicate that environmentally relevant concentrations of BMAA and MCLR enhance activity of the SLC circuit. In addition, these startle sensitivity data reveal NOAELs for BMAA

(100 μM) and MCLR (1 μM), with NOAEL defined as the highest nonstatistically significant dose tested.

BMAA and MCLR Mixture Study: Interaction Among Cyanotoxins at a Behavioral Level

We next aimed to assess whether BMAA and MCLR interact *in vivo* by measuring the effects of a mixture of BMAA and MCLR at their respective NOAELs in larval zebrafish. We exposed wild-type zebrafish embryos from 6 hpf to 6 dpf to 4 different treatment conditions: (1) vehicle controls, (2) 100 μM BMAA, (3) 1 μM
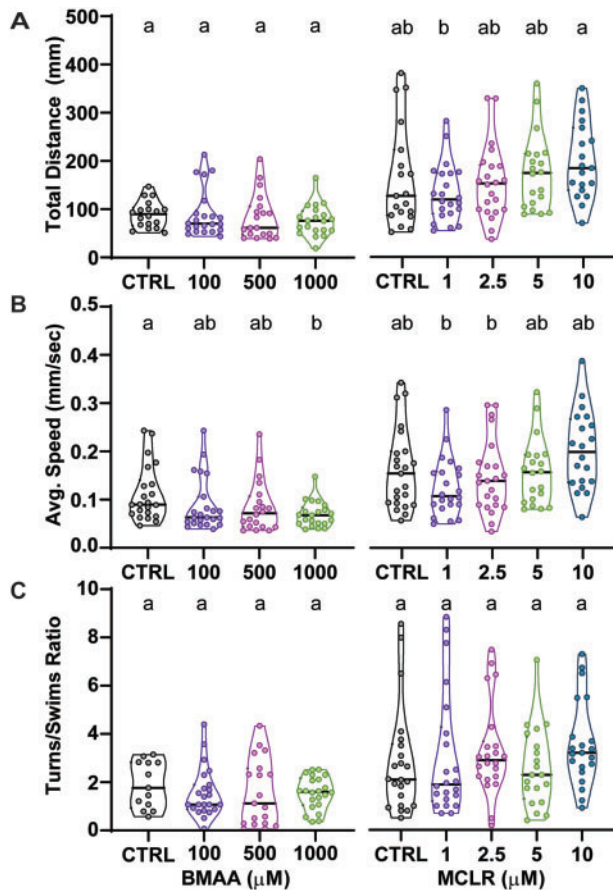
Figure 2. BMAA and MCLR do not substantially alter general locomotor activity. A, Violin plots depict the total distance travelled during the 18.5-min spontaneous movement assay for each larva. B, Average speed across the same assay. C, The ratio of turning movements to swimming movements performed during the spontaneous movement assay. Levels not connected by the same letter are significantly different—Tukey-Kramer HSD, alpha 0.05.

Figure 3. BMAA and MCLR significantly increase acoustic startle sensitivity. A, Startle frequency curves for short-latency C-bends (SLCs, left axis, sigmoidal curve fits) and long-latency C-bends (LLCs, right axis, sigmoidal curve fits) in control larvae (black) and treated larvae (1000 μM BMAA; green). $n = 54$ larvae; mean ± SEM. B and C, SLC and LLC sensitivity indices, calculated for each larva using the curves as in (A). Levels not connected by the same letter are significantly different—Tukey-Kramer HSD, alpha 0.05.

MCLR, and (4) 100 μM BMAA + 1 μM MCLR. As before, no overt developmental or morphological defects were observed in any exposed larvae. We then measured general locomotor activity and sensorimotor function using the same assays described above. In this cohort of animals, 100 μM BMAA very slightly decreased total distance traveled over 18.5 min (Figure 4A), and all 3 treatment groups showed a minor reduction in average speed during the assay (Figure 4B). No differences were observed in turning or swimming behaviors (Figure 4C). These data reinforce the results from our dose-response study that BMAA and MCLR do not substantially alter locomotor activity.

We next measured startle frequency in the same 4 groups of larvae. Figure 4D highlights both the SLC and LLC response frequency disparities between zebrafish larvae exposed to BMAA/MCLR mixture solution (101 μM) and controls. Neither 100 μM BMAA nor 1 μM MCLR altered startle behavior, as both SLC (Figure 4E) and LLC sensitivity indices (Figure 4F) were unchanged. The 101 μM BMAA/MCLR mixture, however, significantly enhanced SLC sensitivity (Figure 4E) while leaving LLC sensitivity unchanged (Figure 4F), in contrast to the effect of BMAA alone (Figure 3). These data demonstrate not only that BMAA and MCLR interact *in vivo* to enhance SLC circuit activity, but because of the different effects of the mixture and the individual toxins on LLC responses (Figure 3C vs. Figure 4F), they
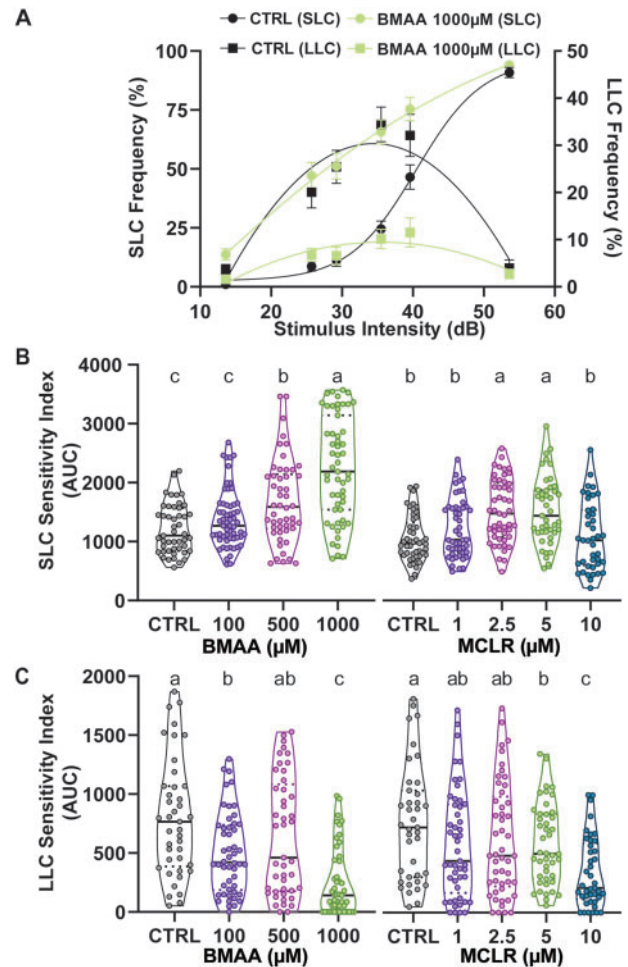
also suggest that different cellular and/or molecular mechanisms are impacted by the mixture.

Global Proteomics Study: Interaction Among Cyanotoxins at a Molecular Level

To explore the molecular underpinnings of these behavioral phenotypes, we performed shotgun proteomics on larval zebrafish exposed to 100 μM BMAA and 1 μM MCLR alone and in combination. After behavioral testing, we carefully collected and flash-froze the treated zebrafish larvae, followed by protein extraction and digestion. Proteomes of larvae for each treatment condition were analyzed by LC-MS/MS, and approximately 3100 proteins were identified in each sample.

DEPs were determined by comparing the mean abundance within treatment to the control group for each protein using a two-way Student-*t* test ($p < .05$) (Tyanova *et al.*, 2016). DEPs in all treatments can be found in Supplementary Tables 2–4. Volcano plots were used to visualize statistically significant differences in protein abundance across treatments in comparison to controls (Supplementary Figure 2). Notably, the BMAA/MCLR
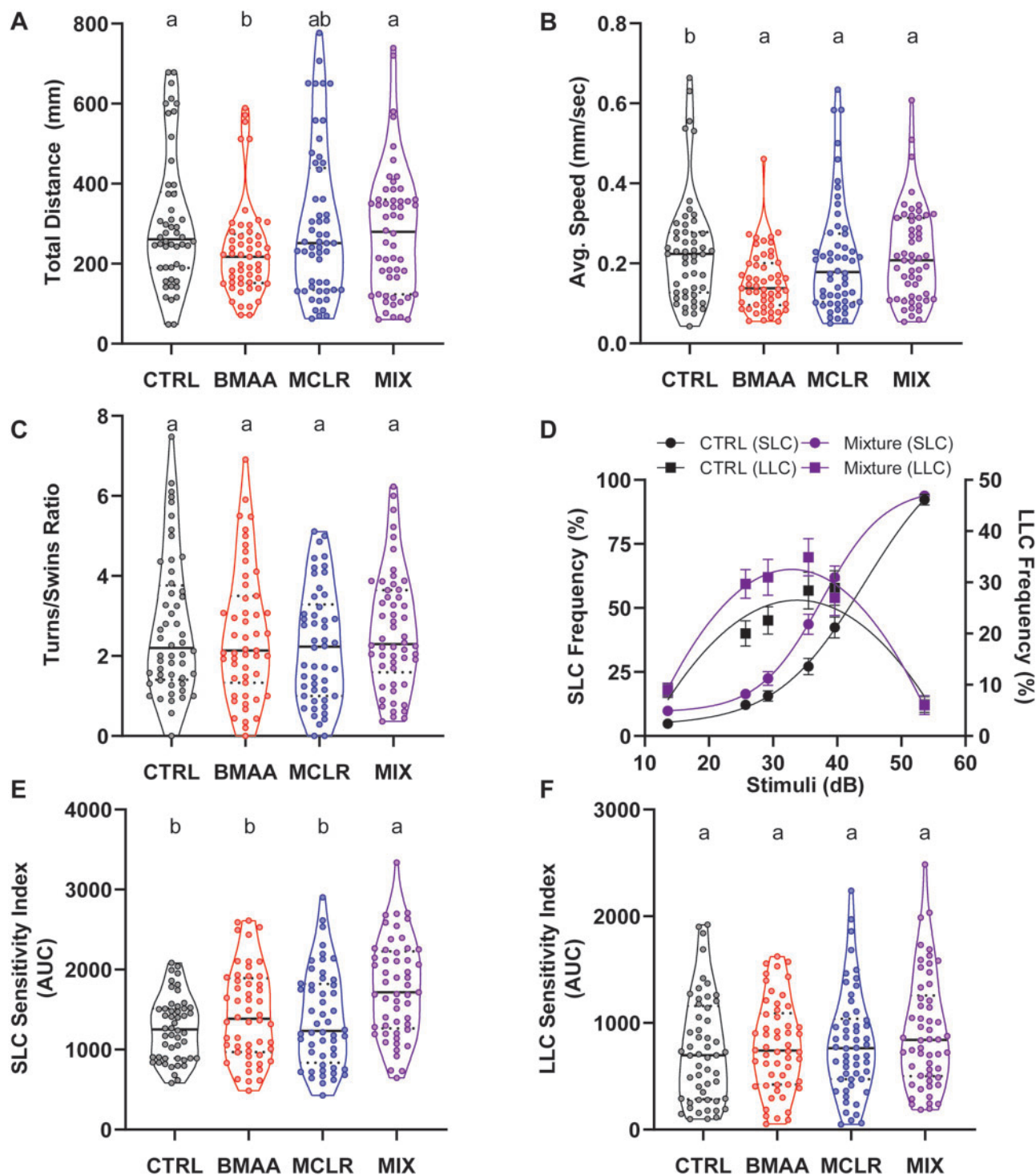
Figure 4. BMAA and MCLR interact to enhance startle sensitivity. A, Violin plots depict the distribution of the total distance travelled during the 18.5-min spontaneous movement assay for each larva. B Violin plot of average speed. (C) Ratio of turns to swims. (D) Startle frequency curves for SLCs (left axis) and LLCs (right axis) in control larvae (0 μM of cyanotoxin, black) and mixture-treated larvae (100 μM BMAA plus 1 μM MCLR, purple). $n = 54$ siblings; mean ± SEM. E and F, SLC and LLC indices for each larva. Levels not connected by the same letter are significantly different–Tukey-Kramer HSD, alpha 0.05.

mixture induced the greatest molecular perturbation, with 259 DEPs compared with 79 for BMAA and 112 for MCLR, representing a 2.5-fold increase for the mixture-exposed group (Figure 5A). Although minimal overlap in DEPs between treatments was observed, we were intrigued by the nine proteins that were significantly differentially expressed in all 3

treatment groups (Figure 5B; Supplementary Table 1). Out of these 9 proteins, 4 proteins were mapped in the enrichment analysis (Table 1), and their general cellular functions include roles in cellular assembly, organization, and development. Interestingly, exposure to the BMAA/MCLR mixture also enhanced the abundance of these 4 DEPs by at least 2.5-fold
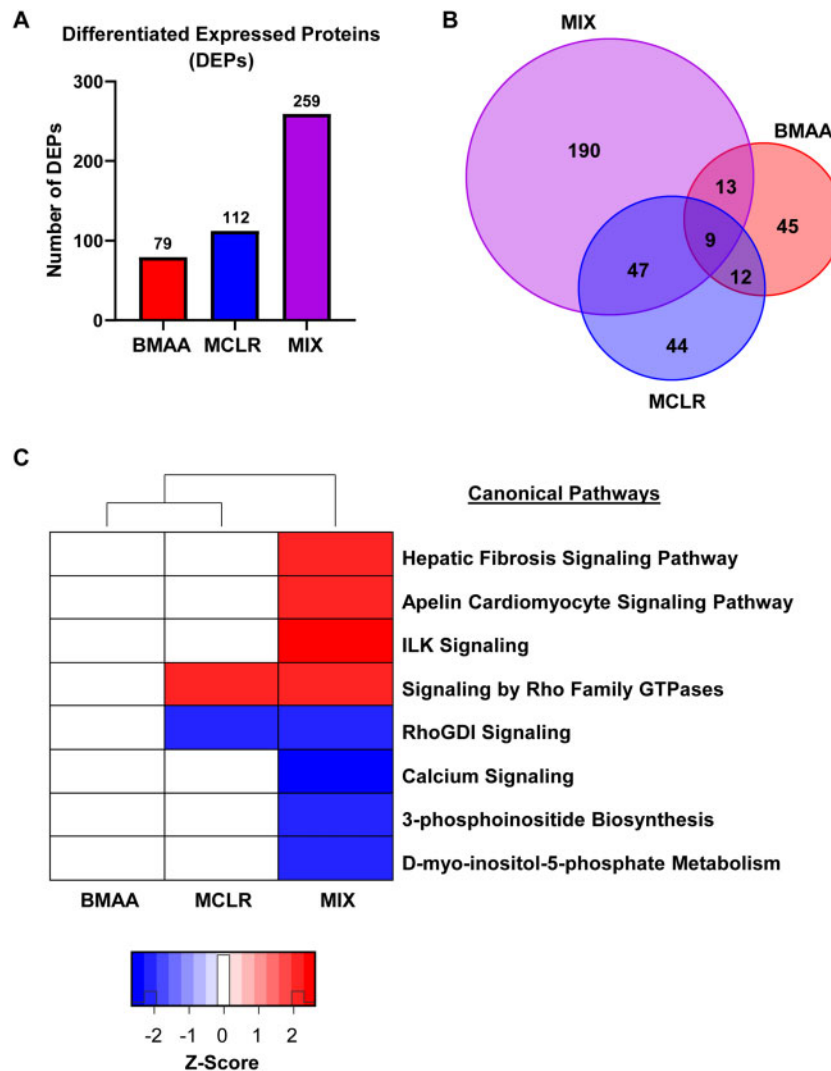
Figure 5. BMAA/MCLR mixture increases protein dysregulation *in vivo*. A, Number of differentially expressed proteins (DEPs) per treatment condition. B Venn diagram showing overlap in DEPs between all treatment groups (red: BMAA protein group, the blue: MCLR protein group, purple: BMAA plus MCLR mixture protein group). C Heat map displaying the impacted canonical pathways from IPA functional analysis. The red or blue-colored rectangles in each column indicates the z-score activities. Red shading indicates predicted activation and blue shading indicates predicted inhibition according to the scale at right. This heat map represents the z-scores obtained from the comparison between significantly expressed proteins ($p \leq .05$).

relative to the individual cyanotoxins. These results reflect an enhanced toxicity after BMAA/MCLR mixture exposure *in vivo*.

To further analyze the identified DEPs across treatments, we performed enrichment analysis to identify significantly perturbed pathways. Supplementary Table 5 lists all canonical pathways found to be significantly perturbed (z-score $\geq |2|$) along with their associated z-scores. Exposure to the BMAA/MCLR mixture enhanced the predicted activation/inhibition of 8 canonical pathways (z-score $\geq |2|$) compared with BMAA (0) and MCLR (2), which supports the observation of a interaction *in vivo* (Figure 5C). RhoGDI signaling (z score = −2.121) and calcium signaling (z score = −2.449) were inhibited, while signaling by Rho Family GTPases (z-score = 2.121) and ILK (z-score = 2.121) were activated. Although exposure to MCLR at 1 μM did not cause behavioral modulation, 2 canonical pathways were significantly affected: (1) inhibition of RhoGDI signaling (z-score = −2) and (2) activation of signaling by Rho family GTPases (z-score = 2) (Figure 5C). All 4 canonical pathways impacted by mixture exposure are broadly associated with neurotoxic

processes related to reorganization of the actin cytoskeleton. Moreover, these pathway analysis results are reinforced by our protein interaction network analysis, in which we found significant differential regulation of key proteins associated with skeletal/muscular disorder and cellular assembly/organization (Supplementary Table 6). Within these networks, key neuronal proteins, including cell division cycle 42 (CDC-42; enrichment p-value = .0049; $\log_2$ fold change = 1.8525), glutamate dehydrogenase 1 (GLUD1; enrichment p-value = .0299; $\log_2$ fold change = 2.6413), and the ALS-associated TDP-43 (TARDBP; ENRICHMENT p-value = 0.0299; $\log_2$ fold change = 2.5508) were significantly upregulated. Because TDP-43 is significantly associated with ALS disease pathology, we looked at expression of TDPBP and TDPBPL in all treatment groups. TDPBP was increased by MCLR exposure, but not BMAA exposure, and this increase was further enhanced by exposure to the BMAA/MCLR mixture (Table 2). Together, these data indicate that BMAA and MCLR in combination impact neurodegenerative processes in larval zebrafish.

Table 1. Shared DEPs Among Treatments

	Protein IDs	Gene Names	*p*-Value	Log$_2$ Fold Change
MCLR	Q4QRD2	*myl4*	0.0029	1.5834
(1 μM)	Q9I8V1	*actc1b*	0.0076	1.2424
	Q7T368	*pdhb*	0.0187	1.0509
	Q6P0V6	*rpl8*	0.0491	0.8516
BMAA	Q6P0V6	*rpl8*	0.0023	−0.892
(100 μM)	Q4QRD2	*myl4*	0.0047	1.0115
	Q9I8V1	*actc1b*	0.033	−0.9068
	Q7T368	*pdhb*	0.0487	−0.9224
Mixture	Q9I8V1	*actc1b*	0.0002	5.3546
(101 μM)	Q4QRD2	*myl4*	0.0135	2.7762
	Q6P0V6	*rpl8*	0.0215	1.6328
	Q7T368	*pdhb*	0.025	2.3007

Table 2. Impact of Cyanotoxin Exposure on TDP Pathway Proteins

	Protein IDs	Gene Names	*p* Value	Log$_2$ Fold Change
BMAA	Q802C7	*tardbp*	0.3614	−1.3194
(100 μM)	Q6NYX2	*tardbpl*	0.9402	0.0674
MCLR	Q802C7	*tardbp*	0.0245	1.6390
(1 μM)	Q6NYX2	*tardbpl*	0.7002	0.5127
Mixture	Q802C7	*tardbp*	0.0159	2.5508
(101 μM)	Q6NYX2	*tardbpl*	0.0520	2.2426

DISCUSSION

Since the 1950s, BMAA has been investigated for its potential to contribute to neurodegenerative diseases, including ALS (Reed et al., 1966). However, BMAA is only one of thousands of toxic metabolites produced by cyanobacteria (Dolman et al., 2012). Although an increasing number of studies have singly addressed BMAA and its adverse effects, major knowledge gaps remain regarding the neuropathological effects of combined exposure to a cocktail of cyanotoxins. A number of studies have reported that cyanotoxins co-occur in natural environments (Banack et al., 2015; Jungblut et al., 2018; Metcalf et al., 2008; Sabart et al., 2015), including BMAA and the most abundant cyanotoxin, MCLR (McKindles et al., 2019). Although first considered to be primarily a hepatotoxin, MCLR has recently been shown to have neurotoxic effects both *in vitro* and *in vivo* (Li et al., 2012, 2015; Wang et al., 2017; Wu et al., 2016). Thus, because BMAA and MCLR are ubiquitously present in the environment, have been previously detected together, and are neurotoxic, our study addresses the important question of whether they interact *in vivo* to enhance adverse effects. Building on prior work demonstrating that cyanotoxins can interact *in vitro* (Main et al., 2018; Martin et al., 2019), we show that (1) both BMAA and MCLR alter the behavior of larval zebrafish (**Figure 3**), (2) a simple binary mixture of BMAA and MCLR at their NOAELs enhances behavioral neurotoxicity (**Figure 4**), and (3) BMAA and MCLR alter molecular changes associated with neuromuscular dysfunction (**Figure 5**).

Larval zebrafish have emerged as a powerful vertebrate model for studying neural development and behavioral circuits, as well as for translational toxicology (Tal et al., 2020; Wolman and Granato, 2012). Although studying larvae is less directly relevant for studies of neurodegeneration, there is increasing evidence that developmental exposures can lead to disease later in life (Heindel and Vandenberg, 2015). Indeed, neonatal exposure to BMAA has been found to cause motor defects and

neurodegeneration in adult rats (Scott et al., 2017; Scott and Downing, 2019). Thus, understanding the developmental impact of cyanotoxin exposure is critical for identifying potential early indicators of degenerative pathology. Here, we show that larval zebrafish behavior is modulated upon exposure to relatively low concentrations of both BMAA and MCLR in a dose-dependent manner. Although only traces of soluble BMAA and MCLR have been found in natural bodies of water (BMAA: 2 μM; MCLR: 0.23 μM) (Wiltsie et al., 2018), BMAA and MCLR can be found at relatively high concentrations (from ~0.02 to 8 mg.kg^{-1} dry weight) in freshwater fish, crustaceans, and other types of seafood (Lance et al., 2018; Sahin et al., 1996) due to bioaccumulation through the food web. Thus, our mixture paradigm is an appropriate model of natural exposures.

Previous studies in larval zebrafish have indicated that BMAA may cause clonus-like convulsions (Purdie et al., 2009) and pericardial edema and altered heart rate (Frøyset et al., 2016; Purdie et al., 2009). We did not observe these effects, but this could be due to differences in strain, embryo medium, exposure route, and analysis methods. In contrast to our data showing no effect on locomotion in bright light conditions (**Figure 2**), MCLR has previously been shown to reduce activity in zebrafish larvae in a light-dark assay (Tzima et al., 2017; Wu et al., 2016). This discrepancy could also arise from strain and media differences, but in agreement with these studies, we did not observe mortality or morphological defects in MCLR-exposed larvae. However, we detected significant, dose-dependent changes in acoustic startle behavior upon exposure to both BMAA and MCLR (**Figure 3**). These data reveal a need for greater standardization in zebrafish rearing methods, and they also show that our acoustic startle assay using high-speed cameras and kinematic analysis may be a broadly useful and highly sensitive addition to standard behavioral neurotoxicity testing.

The increased frequency of Mauthner cell-dependent SLCs in BMAA and MCLR-treated larvae indicates that the underlying sensorimotor circuit is hyperexcitable. BMAA is known to directly agonize glutamatergic receptors (Chiu et al., 2012, 2013), so the startle hypersensitivity in BMAA-treated fish could reflect that startle circuit neurons fire more easily following acoustic stimuli. Alternatively, hypersensitivity from exposure to these cyanotoxins could result from a reduction in inhibitory control of the startle circuit. Interestingly, both of these mechanisms have implications for ALS pathology, as excitotoxicity either from direct overstimulation of excitatory pathways, or from a loss of inhibitory input have been implicated in motor neuron death (Martin et al., 2012). Furthermore, our data show that BMAA and MCLR interact to enhance startle sensitivity at their respective NOAELs (**Figure 4**). This greater-than-additive effect strongly suggests a synergistic interaction between BMAA and MCLR (Greco et al., 1996), but defining synergy often requires testing an array of binary mixture ratios (McCarty and Borgert, 2006; Roell et al., 2017). Thus, further analysis is needed to precisely define the nature of the BMAA/MCLR interaction. To the best of our knowledge, only one previous study has examined the effects of exposure to BMAA and MCLR as a mixture. Anxiety-like behavior, exploratory behavior, and general locomotion were all found to be unchanged by acute exposure to a BMAA/MCLR mixture in the adult C57BL/6 mouse model (Myhre et al., 2018). This could indicate that the effects of the BMAA/MCLR mixture are limited to specific brain circuits, and/or that these neurotoxins exert their effects more strongly during early developmental stages (Karlsson et al., 2012; Scott et al., 2017). Future studies will examine the long-term effects of developmental exposure to BMAA and MCLR.

To understand how BMAA and MCLR drive neurotoxicity, we used a label-free proteomics approach to identify the molecular pathways disrupted by BMAA/MCLR exposure in larval zebrafish. Our proteomics data display a clear trend toward enhanced toxicity in the mixture exposed group versus single exposures (Figure 5A), further supporting the conclusion from our behavioral data that the two toxins interact *in vivo*. Interestingly, DEPs displayed minimal overlap between treatments (Figure 5B), suggesting they act through different modes of action. It is notable that the BMAA/MCLR mixture impacted multiple critical cellular pathways, including signaling by ILK, Rho Family GTPases, RhoGDI, and calcium (Figure 5C), which all impinge on regulation of the actin cytoskeleton. For example, overexpression of proteins in the Rho Family GTPase pathway such as CDC42 has specific effects on the actin filamentous system (Nobes and Hall, 1995). CDC42 has a well-established role in triggering the formation/assembly of stress fibers mediated by Arp2/3-dependent actin nucleation (Aspenström, 2019). These data are consistent with prior work showing that loss-of-function mutations in *cytoplasmic FMRP-interacting protein 2* (*cyfip2*), a key regulator of Arp2/3-mediated actin polymerization, cause startle hypersensitivity in larval zebrafish similar to that seen with BMAA/MCLR exposure (Marsden *et al.*, 2018). In addition, previous reports show that MCLR induces neurotoxicity by triggering reorganization of actin cytoskeleton components (Li *et al.*, 2012; Meng *et al.*, 2011) by inhibiting serine/threonine-specific protein phosphatases (PPs) 1 and 2 A (Huynh-Delerme *et al.*, 2005; MacKintosh *et al.*, 1990). Here, we show here that MCLR in combination with BMAA at low concentrations inhibits expression of these same protein PPs associated with cytoskeletal organization (PP1CAB [Q7ZVR3], enrichment p-value = .0106; $\log_2$ fold change = −2.476; PP2CA [F1Q6Z7], enrichment p-value = .0110; $\log_2$ fold change = −4.03; Supplementary Table 3). Together, our molecular proteomics data support the idea that acoustic startle hypersensitivity may be an early indicator of neuronal stress.

That our unbiased proteomic analysis also revealed an upregulation of TDP-43 in BMAA/MCLR-exposed larvae (Table 2, Supplementary Table 6) is particularly striking. Cytoplasmatic TDP-43 inclusions are the key pathological hallmark in 98% of sALS cases (Mackenzie *et al.*, 2010). Although our results cannot verify the sub-cellular localization of upregulated TDP-43, previous reports have shown that overexpression of TDP-43 in the cytoplasm leads to depletion of nuclear TDP-43, which has detrimental effects in mice (Fratta *et al.*, 2018; Wils *et al.*, 2010). Although MCLR—but not BMAA—exposure also increased TDP-43 expression, this increase was exacerbated by the mixture, indicating that exposure to multiple cyanotoxins may enhance sALS disease processes. Although the molecular mechanisms that specifically drive cyanotoxin-mediated neurotoxicity are not fully understood, our data support a model in which cyanotoxin mixtures cause neural dysfunction through multiple disease-associated pathways.

Together, our data provide new evidence that cyanotoxins interact *in vivo* to cause changes not only at the molecular level but also at the whole-organism level, as demonstrated by altered behavioral performance. Future work will seek to link specific molecular pathways, behavior regulation, and neuronal dysfunction, with the goal of revealing novel therapeutic and/or diagnostic targets for intractable neurodegenerative diseases such as ALS.

SUPPLEMENTARY DATA

Supplementary data are available at *Toxicological Sciences* online.

DECLARATION OF CONFLICTING INTERESTS

The authors declared no potential conflicts of interest with respect to the research, authorship, and/or publication of this article.

REFERENCES

Aspenström, P. (2019). The intrinsic GDP/GTP exchange activities of Cdc42 and rac1 are critical determinants for their specific effects on mobilization of the actin filament system. *Cells* **8**, 759.

Banack, S. A., Caller, T., Henegan, P., Haney, J., Murby, A., Metcalf, J. S., Powell, J., Cox, P. A., and Stommel, E. (2015). Detection of cyanotoxins, β-n-methylamino-l-alanine and microcystins, from a lake surrounded by cases of amyotrophic lateral sclerosis. *Toxins* **7**, 322–336.

Banack, S. A., and Cox, P. A. (2003). Distribution of the neurotoxic nonprotein amino acid BMAA in *Cycas micronesica*. *Bot. J. Linn. Soc.* **143**, 165–168.

Bereman, M. S., Beri, J., Enders, J. R., and Nash, T. (2018). Machine learning reveals protein signatures in CSF and plasma fluids of clinical value for ALS. *Sci. Rep.* **8**, 16334.

Beri, J., Nash, T., Martin, R. M., and Bereman, M. S. (2017). Exposure to BMAA mirrors molecular processes linked to neurodegenerative disease. *Proteomics* **17**, 1700161.

Bozzoni, V. (2016). Amyotrophic lateral sclerosis and environmental factors. *Funct. Neurol.* **31**, 7.

Bradley, W. G., and Mash, D. C. (2009). Beyond guam: The cyanobacteria/BMAA hypothesis of the cause of ALS and other neurodegenerative diseases. *Amyotroph. Lateral Scler.* **10**, 7–20.

Brown, R. H., and Al-Chalabi, A. (2017). Amyotrophic lateral sclerosis. *N. Engl. J. Med.* **377**, 162–172.

Burgess, H. A., and Granato, M. (2007). Modulation of locomotor activity in larval zebrafish during light adaptation. *J. Exp. Biol.* **210**, 2526–2539.

Caller, T. A., Doolin, J. W., Haney, J. F., Murby, A. J., West, K. G., Farrar, H. E., Ball, A., Harris, B. T., and Stommel, E. W. (2009). A cluster of amyotrophic lateral sclerosis in New Hampshire: A possible role for toxic cyanobacteria blooms. *Amyotroph. Lateral Scler.* **10**, 101–108.

Chiu, A. S., Gehringer, M. M., Braidy, N., Guillemin, G. J., Welch, J. H., and Neilan, B. A. (2012). Excitotoxic potential of the cyanotoxin β-methyl-amino-l-alanine (BMAA) in primary human neurons. *Toxicon* **60**, 1159–1165.

Chiu, A. S., Gehringer, M. M., Braidy, N., Guillemin, G. J., Welch, J. H., and Neilan, B. A. (2013). Gliotoxicity of the cyanotoxin, β-methyl-amino-l-alanine (BMAA). *Sci. Rep.* **3**, 1482–1482.

Ciura, S., Lattante, S., Le Ber, I., Latouche, M., Tostivint, H., Brice, A., and Kabashi, E. (2013). Loss of function of c9orf72 causes motor deficits in a zebrafish model of amyotrophic lateral sclerosis. *Ann. Neurol.* **74**, 180–187.

Cox, P. A., Banack, S. A., Murch, S. J., Rasmussen, U., Tien, G., Bidigare, R. R., Metcalf, J. S., Morrison, L. F., Codd, G. A., and Bergman, B. (2005). Diverse taxa of cyanobacteria produce β-n-methylamino-l-alanine, a neurotoxic amino acid. *Proc. Nat. Acad. Sci. U.S.A.* **102**, 5074–5078.

Dolman, A. M., Rücker, J., Pick, F. R., Fastner, J., Rohrlack, T., Mischke, U., and Wiedner, C. (2012). Cyanobacteria and cyanotoxins: The influence of nitrogen versus phosphorus. *PLoS One* **7**, e38757.

Field, N. C., Metcalf, J. S., Caller, T. A., Banack, S. A., Cox, P. A., and Stommel, E. W. (2013). Linking β-methylamino-l-alanine exposure to sporadic amyotrophic lateral sclerosis in Annapolis, MD. *Toxicon* **70**, 179–183.

Fratta, P., Sivakumar, P., Humphrey, J., Lo, K., Ricketts, T., Oliveira, H., Brito-Armas, J. M., Kalmar, B., Ule, A., Yu, Y., *et al.* (2018). Mice with endogenous tdp-43 mutations exhibit gain of splicing function and characteristics of amyotrophic lateral sclerosis. *EMBO J.* **37**, e98684.

Frøyset, A. K., Khan, E. A., and Fladmark, K. E. (2016). Quantitative proteomics analysis of zebrafish exposed to sub-lethal dosages of β-methyl-amino-l-alanine (BMAA). *Sci. Rep.* **6**, 29631.

Greco, N. J., Jones, G. D., Tandon, N. N., Kornhauser, R., Jackson, B., and Jamieson, G. A. (1996). Differentiation of the two forms of GPIB functioning as receptors for α-thrombin and von Willebrand factor: Ca2+ responses of protease-treated human platelets activated with α-thrombin and the tethered ligand peptide. *Biochemistry* **35**, 915–921.

Hao, L. T., Wolman, M., Granato, M., and Beattie, C. E. (2012). Survival motor neuron affects plastin 3 protein levels leading to motor defects. *J. Neurosci.* **32**, 5074–5084.

Heindel, J. J., and Vandenberg, L. N. (2015). Developmental origins of health and disease: A paradigm for understanding disease cause and prevention. *Curr. Opin. Pediatr.* **27**, 248–253.

Huynh-Delerme, C., Edery, M., Huet, H., Puiseux-Dao, S., Bernard, C., Fontaine, J.-J., Crespeau, F., and de Luze, A. (2005). Microcystin-lr and embryo–larval development of medaka fish, *Oryzias latipes*. I. Effects on the digestive tract and associated systems. *Toxicon* **46**, 16–23.

Ingre, C., Roos, P. M., Piehl, F., Kamel, F., and Fang, F. (2015). Risk factors for amyotrophic lateral sclerosis. *Clinical Epidemiol.* **7**, 181–193.

Jones, N. (2009). Genetic risk factors for sporadic ALS. *Nat. Rev. Neurol.* **5**, 579.

Jungblut, A. D., Wilbraham, J., Banack, S. A., Metcalf, J. S., and Codd, G. A. (2018). Microcystins, BMAA and BMAA isomers in 100-year-old Antarctic cyanobacterial mats collected during Captain R. F. Scott's Discovery expedition. *Eur. J. Phycol.* **53**, 115–121.

Karlsson, O., Berg, A.-L., Lindström, A.-K., Hanrieder, J., Arnerup, G., Roman, E., Bergquist, J., Lindquist, N. G., Brittebo, E. B., and Andersson, M. (2012). Neonatal exposure to the cyanobacterial toxin BMAA induces changes in protein expression and neurodegeneration in adult hippocampus. *Toxicol. Sci.* **130**, 391–404.

Karlsson, O., Michno, W., Ransome, Y., and Hanrieder, J. (2017). MALDI imaging delineates hippocampal glycosphingolipid changes associated with neurotoxin induced proteopathy following neonatal BMAA exposure. *Biochim. Biophys. Acta* **1865**, 740–746.

Khatri, P., and Drăghici, S. (2005). Ontological analysis of gene expression data: Current tools, limitations, and open problems. *Bioinformatics* **21**, 3587–3595.

Kurland, L. T., and Mulder, D. W. (1955). Epidemiologic investigations of amyotrophic lateral sclerosis. 2. Familial aggregations indicative of dominant inheritance. II. *Neurology* **5**, 249–249.

Lance, E., Arnich, N., Maignien, T., and Biré, R. (2018). Occurrence of β-n-methylamino-l-alanine (BMAA) and isomers in aquatic environments and aquatic food sources for humans. *Toxins* **10**, 83.

Li, G., Cai, F., Yan, W., Li, C., and Wang, J. (2012). A proteomic analysis of MCLR-induced neurotoxicity: Implications for Alzheimer's disease. *Toxicol. Sci.* **127**, 485–495.

Li, G., Yan, W., Dang, Y., Li, J., Liu, C., and Wang, J. (2015). The role of calcineurin signaling in microcystin-LR triggered neuronal toxicity. *Sci. Rep.* **5**, 11271.

Li, Y., Ye, H., Du, M., Zhang, Y., Ye, B., Pu, Y., and Wang, D. (2009). Induction of chemotaxis to sodium chloride and diacetyl and thermotaxis defects by microcystin-LR exposure in nematode *Caenorhabditis elegans*. *J. Environ. Sci.* **21**, 971–979.

Lobner, D., Piana, P. M. T., Salous, A. K., and Peoples, R. W. (2007). B-N-methylamino-L-alanine enhances neurotoxicity through multiple mechanisms. *Neurobiol. Dis.* **25**, 360–366.

Mackenzie, I. R., Rademakers, R., and Neumann, M. (2010). TDP-43 and FUS in amyotrophic lateral sclerosis and frontotemporal dementia. *Lancet Neurol.* **9**, 995–1007.

MacKintosh, C., Beattie, K. A., Klumpp, S., Cohen, P., and Codd, G. A. (1990). Cyanobacterial microcystin-LR is a potent and specific inhibitor of protein phosphatases 1 and 2a from both mammals and higher plants. *FEBS Lett.* **264**, 187–192.

Main, B. J., Main, B. J., Rodgers, K. J., and Rodgers, K. J. (2018). Assessing the combined toxicity of BMAA and its isomers 2,4-DAB and AEG in vitro using human neuroblastoma cells. *Neurotox. Res.* **33**, 33–42.

Marquart, G. D., Tabor, K. M., Bergeron, S. A., Briggman, K. L., and Burgess, H. A. (2019). Prepontine non-giant neurons drive flexible escape behavior in zebrafish. *PLoS Biol.* **17**, e3000480.

Marsden, K. C., Jain, R. A., Wolman, M. A., Echeverry, F. A., Nelson, J. C., Hayer, K. E., Miltenberg, B., Pereda, A. E., and Granato, M. (2018). A cyfip2-dependent excitatory interneuron pathway establishes the innate startle threshold. *Cell Rep.* **23**, 878–887.

Martin, L. J., Martin, L. J., Chang, Q., and Chang, Q. (2012). Inhibitory synaptic regulation of motoneurons: A new target of disease mechanisms in amyotrophic lateral sclerosis. *Mol. Neurobiol.* **45**, 30–42.

Martin, R. M., Stallrich, J., and Bereman, M. S. (2019). Mixture designs to investigate adverse effects upon co-exposure to environmental cyanotoxins. *Toxicology* **421**, 74–83.

Masseret, E., Banack, S., Boumédiène, F., Abadie, E., Brient, L., Pernet, F., Juntas-Morales, R., Pageot, N., Metcalf, J., Cox, P., *et al.* (2013). Dietary BMAA exposure in an amyotrophic lateral sclerosis cluster from southern France. *PLoS One* **8**, e83406.

McCarty, L. S., and Borgert, C. J. (2006). Review of the toxicity of chemical mixtures: Theory, policy, and regulatory practice. *Regula. Toxicol. Pharmacol.* **45**, 119–143.

McGown, A., McDearmid, J. R., Panagiotaki, N., Tong, H., Al Mashhadi, S., Redhead, N., Lyon, A. N., Beattie, C. E., Shaw, P. J., and Ramesh, T. M. (2013). Early interneuron dysfunction in

ALS: Insights from a mutant sod1 zebrafish model. *Ann. Neurol.* **73**, 246–258.

McKindles, K. M., Zimba, P. V., Chiu, A. S., Watson, S. B., Gutierrez, D. B., Westrick, J., Kling, H., and Davis, T. W. (2019). A multiplex analysis of potentially toxic cyanobacteria in Lake Winnipeg during the 2013 bloom season. *Toxins* **11**, 587.

Meng, G., Sun, Y., Fu, W., Guo, Z., and Xu, L. (2011). Microcystin-LR induces cytoskeleton system reorganization through hyperphosphorylation of tau and HSP27 via PP2A Inhibition and Subsequent Activation of the p38 MAPK signaling pathway in neuroendocrine (PC12) cells. *Toxicology* **290**, 218–229.

Metcalf, J. S., Banack, S. A., Lindsay, J., Morrison, L. F., Cox, P. A., and Codd, G. A. (2008). Co-occurrence of β-n-methylamino-l-alanine, a neurotoxic amino acid with other cyanobacterial toxins in British waterbodies, 1990–2004. *Agris* **10**, 702–708.

Metcalf, J. S., Richer, R., Cox, P. A., and Codd, G. A. (2012). Cyanotoxins in desert environments may present a risk to human health. *Sci. Total Environ.* **421–422**, 118–123.

Myhre, O., Eide, D. M., Kleiven, S., Utkilen, H. C., and Hofer, T. (2018). Repeated five-day administration of l-BMAA, microcystin-LR, or as mixture, in adult c57bl/6 mice – lack of adverse cognitive effects. *Sci. Rep.* **8**, 2308–2314.

Nobes, C. D., and Hall, A. (1995). Rho, rac, and cdc42 GTPases regulate the assembly of multimolecular focal complexes associated with actin stress fibers, lamellipodia, and filopodia. *Cell* **81**, 53–62.

Pašková, V., Adamovský, O., Pikula, J., Skočovská, B., Band'ouchová, H., Horáková, J., Babica, P., Maršálek, B., and Hilscherová, K. (2008). Detoxification and oxidative stress responses along with microcystins accumulation in Japanese quail exposed to cyanobacterial biomass. *Sci. Total Environ.* **398**, 34–47.

Purdie, E. L., Samsudin, S., Eddy, F. B., and Codd, G. A. (2009). Effects of the cyanobacterial neurotoxin β-n-methylamino-l-alanine on the early-life stage development of zebrafish (*Danio rerio*). *Aquatic Toxicology* **95**, 279–284.

Ramesh, T., Lyon, A. N., Pineda, R. H., Wang, C., Janssen, P. M., Canan, B. D., Burghes, A. H., and Beattie, C. E. (2010). A genetic model of amyotrophic lateral sclerosis in zebrafish displays phenotypic hallmarks of motoneuron disease. *Dis. Model. Mech.* **3**, 652–662.

Reed, D., Plato, C., Elizan, T., and Kurland, L. T. (1966). The amyotrophic lateral sclerosis/parkinsonism-dementia complex: A ten-year follow-up on guam. I. Epidemiologic studies. *Am. J. Epdemiol.* **83**, 54–73.

Renton, A. E., Chiò, A., and Traynor, B. J. (2014). State of play in amyotrophic lateral sclerosis genetics. *Nat. Neurosci.* **17**, 17–23.

Roell, K. R., Reif, D. M., and Motsinger-Reif, A. A. (2017). An introduction to terminology and methodology of chemical synergy-perspectives from across disciplines. *Front. Pharmacol.* **8**, 158.

Sabart, M., Crenn, K., Perrière, F., Abila, A., Leremboure, M., Colombet, J., Jousse, C., and Latour, D. (2015). Co-occurrence of microcystin and anatoxin-a in the freshwater lake Aydat (France): Analytical and molecular approaches during a three-year survey. *Harmful Algae* **48**, 12–20.

Sahin, A., Tencalla, F. G., Dietrich, D. R., and Naegeli, H. (1996). Biliary excretion of biochemically active cyanobacteria (blue-green algae) hepatotoxins in fish. *Toxicology* **106**, 123–130.

Scott, L., and Downing, T. (2019). Dose-dependent adult neurodegeneration in a rat model after neonatal exposure to β-n-methylamino-l-alanine. *Neurotox. Res.* **35**, 711–723.

Scott, L. L., Downing, T. G., Timothy, D., and Laura, S. (2017). A single neonatal exposure to BMAA in a rat model produces neuropathology consistent with neurodegenerative diseases. *Toxins* **10**, 22.

Swinnen, B., and Robberecht, W. (2014). The phenotypic variability of amyotrophic lateral sclerosis. *Nat. Rev. Neurol.* **10**, 661–670.

Tal, T., Yaghoobi, B., and Lein, P. J. (2020). Translational toxicology in zebrafish. *Curr. Opin. Toxicol.* **23–24**, 56–66.

Tao, Q.-Q., Wei, Q., and Wu, Z.-Y. (2018). Sensory nerve disturbance in amyotrophic lateral sclerosis. *Life Sci.* **203**, 242–245.

Tyanova, S., Temu, T., Sinitcyn, P., Carlson, A., Hein, M. Y., Geiger, T., Mann, M., and Cox, J. (2016). The perseus computational platform for comprehensive analysis of (prote)omics data. *Nat. Methods* **13**, 731–740.

Tzima, E., Serifi, I., Tsikari, I., Alzualde, A., Leonardos, I., and Papamarcaki, T. (2017). Transcriptional and behavioral responses of zebrafish larvae to microcystin-lr exposure. *Int. J. Mol. Sci.* **18**, 365.

Wang, B., Liu, J., Huang, P., Xu, K., Wang, H., Wang, X., Guo, Z., and Xu, L. (2017). Protein phosphatase 2a inhibition and subsequent cytoskeleton reorganization contributes to cell migration caused by microcystin-LR in human laryngeal epithelial cells (Hep-2). *Environ. Toxicol.* **32**, 890–903.

Wang, Q., Xie, P., Chen, J., and Liang, G. (2008). Distribution of microcystins in various organs (heart, liver, intestine, gonad, brain, kidney and lung) of Wistar rat via intravenous injection. *Toxicon* **52**, 721–727.

Wils, H., Kleinberger, G., Janssens, J., Pereson, S., Joris, G., Cuijt, I., Smits, V., Ceuterick-de Groote, C., Van Broeckhoven, C., and Kumar-Singh, S. (2010). Tdp-43 transgenic mice develop spastic paralysis and neuronal inclusions characteristic of ALS and frontotemporal lobar degeneration. *Proc. Natl. Acad. Sci. U.S.A.* **107**, 3858–3863.

Wiltsie, D., Schnetzer, A., Green, J., Vander Borgh, M., and Fensin, E. (2018). Algal blooms and cyanotoxins in Jordan Lake, North Carolina. *Toxins* **10**, 92.

Wolman, M., and Granato, M. (2012). *Behavioral Genetics in Larval Zebrafish: Learning from the Young*, pp. 366–372. Wiley Subscription Services, Inc., A Wiley Company, Hoboken.

Wu, Q., Yan, W., Liu, C., Li, L., Yu, L., Zhao, S., and Li, G. (2016). Microcystin-LR exposure induces developmental neurotoxicity in zebrafish embryo. *Environ. Pollut.* **213**, 793–800.

Zhao, S., Li, G., and Chen, J. (2015). A proteomic analysis of prenatal transfer of microcystin-LR induced neurotoxicity in rat offspring. *J. Proteomics* **114**, 197–213.